Inorganic Chemistry
Article

Inorg. Chem. **2010**, *49*, 4331–4342 **4331**
DOI: 10.1021/ic100300y

Synthesis, Characterization, and Catalytic Properties of New Electrophilic Iridium(III) Complexes Containing the (*R*)-(+)-2,2′-Bis(diphenylphosphino)-1,1′-binaphthyl Ligand

Abdurrahman C. Atesin, Jing Zhang, Tulaza Vaidya, William W. Brennessel, Alison J. Frontier,* and Richard Eisenberg*

Department of Chemistry, University of Rochester, Rochester, New York 14627

Received February 12, 2010

The oxidative addition of MeI to the Ir(I) square-planar complex IrI(CO)((*R*)-(+)-BINAP) where (*R*)-(+)-BINAP = (*R*)-(+)-2,2′-bis(diphenylphosphino)-1,1′-binaphthyl)) results in the formation of two diastereomers in a 2:1 ratio of the Ir(III) oxidative addition product $IrI_2(CO)(Me)((R)$-(+)-BINAP) (**4a** and **4b**) in a 85% overall yield. Upon iodide abstraction from the diastereomeric mixture with 2 equiv of $AgSbF_6$ in the presence of diethyl isopropylidene malonate (DIM), two diastereomers of the dicationic complex $[Ir(CO)(Me)(DIM)((R)$-(+)-BINAP)$][SbF_6]_2$ (**5**) are formed in a 90% yield with a ratio of 9:1. One diastereomer of the diiodide complex **4** and one diastereomer of the dicationic complex **5** have been characterized by X-ray diffraction. An anion exchange reaction of **5** with $NaBAr_4^{f-}$ (BAr_4^{f-} = $B(3,5\text{-}(CF_3)_2C_6H_3)_4$) affords $[Ir(CO)(Me)(DIM)$-$((R)$-(+)-BINAP)$][BAr_4^f]_2$ (**6**) in quantitative yield. Both **5** and **6** are active Lewis acid catalysts for the polarized Nazarov cyclization and the Diels−Alder reaction. In the Nazarov cyclization, when $NaBAr_4^f$ is added as a cofactor for the reaction catalyzed by **5** or **6**, the resultant oxyallyl cation intermediate from the 4π conrotation undergoes a Wagner−Meerwein rearrangement to afford spirocyclic cyclopentenones in modest to good yields.

Introduction

Electrophilicly driven reactions promoted by cationic complexes of the platinum group elements in nonpolar, aprotic media comprise an important class of transition metal catalyzed reactions. Recent developments in the electrophilic chemistry of platinum group metal complexes include catalysis of α-olefin polymerization by cationic palladium(II) systems and C−H bond activation using cationic platinum(II) and iridium(III) complexes.[1] In the majority of these studies, the metal complexes have an alkyl ligand and at least one labile binding site occupied by a weakly coordinating solvent molecule. Charge is balanced in these systems by essentially non-coordinating anions. Over the past decade, research by Eisenberg and coworkers have focused on the development of cationic iridium(III) complexes fulfilling these criteria with adjacent coordination sites occupied by readily dissociatable chelating ligands that allow for substrate activation through coordination and possibly chelation to the metal center. In the course of developing such reactive systems, the d^6 iridium(III) dicationic complex $[Ir(Me)(CO)(dppe)(DIB)][BAr^f_4]_2$, **1** (dppe = 1,2-bis(diphenylphosphino)ethane, DIB = 1, 2-diiodobenzene and $BAr^f_4{}^-$ = $B(3,5\text{-}(CF_3)_2C_6H_3)_4$) was prepared and fully characterized.[2]

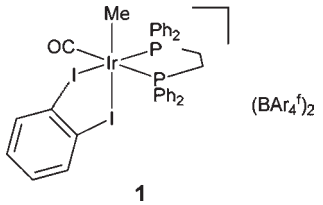

1

Complex **1** exhibited electrophilic behavior leading to the initiation of cationic polymerization or oligomerization of different electron-rich olefins.[2,3] Subsequently, **1** was found to be an efficient catalyst for promoting Nazarov cyclization

*To whom correspondence should be addressed. E-mail: eisenberg@chem.rochester.edu (R.E.).

(1) (a) Ittel, S. D.; Johnson, L. K.; Brookhart, M. *Chem. Rev.* **2000**, *100*, 1169. (b) Johnson, L. K.; Killian, C. M.; Brookhart, M. J. *J. Am. Chem. Soc.* **1995**, *117*, 6414. (c) Gibson, V. C.; Spitzmesser, S. K. *Chem. Rev.* **2003**, *103*, 283. (d) Drent, E.; Budzelaar, P. H. M. *Chem. Rev.* **1996**, *96*, 663. (e) Rix, F. C.; Brookhart, M.; White, P. S. *J. Am. Chem. Soc.* **1996**, *118*, 4746. (f) Arndtsen, B. A.; Bergman, R. G. *Science* **1995**, *270*, 1970. (g) Tellers, D. M.; Bergman, R. G. *J. Am. Chem. Soc.* **2000**, *122*, 954. (h) Tellers, D. M.; Bergman, R. G. *Organometallics* **2001**, *20*, 4819. (i) Golden, J. T.; Andersen, R. A.; Bergman, R. G. *J. Am. Chem. Soc.* **2001**, *123*, 5837. (j) Tellers, D. M.; Yung, C. M.; Arndtsen, B. A.; Adamson, D. R.; Bergman, R. G. *J. Am. Chem. Soc.* **2002**, *124*, 1400. (k) Holtcamp, M. W.; Labinger, J. A.; Bercaw, J. E. *J. Am. Chem. Soc.* **1997**, *119*, 848. (l) Johansson, L.; Tilset, M.; Labinger, J. A.; Bercaw, J. E. *J. Am. Chem. Soc.* **2000**, *122*, 10846. (m) Johansson, L.; Ryan, O. B.; Tilset, M. *J. Am. Chem. Soc.* **1999**, *121*, 1974. (n) Labinger, J. A.; Bercaw, J. E. *Nature* **2002**, *417*, 507. (o) Wik, B. J.; Lersch, M.; Tilset, M. *J. Am. Chem. Soc.* **2002**, *124*, 12116. (p) Clot, E.; Chen, J.; Lee, D.-H.; Sung, S. Y.; Appelhans, L. N.; Faller, J. W.; Crabtree, R. H.; Eisenstein, O. *J. Am. Chem. Soc.* **2004**, *126*, 8795. (q) Song, D.; Jia, W. L.; Wang, S. *Organometallics* **2004**, *23*, 1194. (r) Williams, T. J.; Caffyn, A. J. M.; Hazari, N.; Oblad, P. F.; Labinger, J. A.; Bercaw, J. E. *J. Am. Chem. Soc.* **2008**, *130*, 2418. (s) Guan, Z.; Popeney, C. S. In *Topics in Organometallics Chemistry*; Springer GmbH: New York, 2009; Vol. *26*, p 179.

(2) Albietz, P. J.; Cleary, B. P.; Paw, W.; Eisenberg, R. *J. Am. Chem. Soc.* **2001**, *123*, 12091.

(3) Albietz, P. J.; Cleary, B. P.; Paw, W.; Eisenberg, R. *Inorg. Chem.* **2002**, *41*, 2095.

Published on Web 04/02/2010

Scheme 1

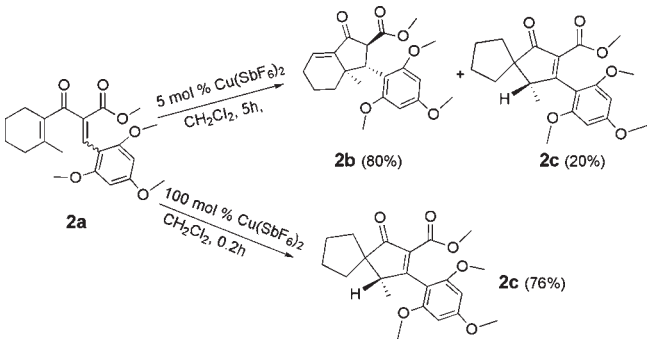

of polarized aryl vinyl and divinyl ketones to form five-membered carbocycles,[4] as well as a tandem reaction sequences involving Nazarov cyclization and subsequent Michael addition under mild conditions at substantially higher rates than other Lewis acid catalysts.[5]

Within the past decade interest in the polarized Nazarov cyclization has attracted considerable attention because of the reaction's potential application in the synthesis of natural products and bioactive molecules containing highly functionalized five-membered carbocycles. Catalysis of Nazarov cyclization has been reported with simple transition metal complexes such as $Cu(OTf)_2$,[6] $Sc(OTf)_3$,[7] $Pd(MeCN)_2Cl_2$,[8] $Cu(SbF_6)_2$,[9] $Fe(ClO_4)_3 \cdot Al_2O_3$,[10] and $V(salen)Cl_2/AgSbF_6$ in good to excellent yields.[11] For derivatives of these catalysts to which a chelating *chiral* ligand has been added, moderate to good enantioselectivities have been reported, such as with $Sc(pybox)(OTf)_3$,[12] $Cu(pybox)(OTf)_2$,[13] and Ni(bis{(*R*)-1-[(*S*)-2-(diphenylphosphino)ferrocenyl]ethyl}-cyclohexylphosphine)(THF)][ClO_4]$_2$.[14]

In a study by Huang and Frontier reported in 2007,[9] when substrate **2a** (Scheme 1) was treated with *stoichiometric* amounts of $Cu(SbF_6)_2$, an unusual spirocycle product **2c** was obtained in good yield, while in other reactions with a catalytic amount of the metal promoter, only a mixture of the spirocycle product **2c** and the Nazarov product **2b** were observed to form, with the ratio favoring **2b**. It was proposed that the spirocycle forms through a Wagner−Meerwein rearrangement of the intermediate carbocation generated in the reaction sequence. These observations, along with the high substrate reactivity observed for the Ir(III) cationic complex **1** suggested that **1** might catalyze the reaction of **2a** to form the spirocycle product **2c** under appropriate conditions. Additionally, through the use of a chiral analogue of **1**, it was hypothesized that asymmetric induction could be achieved.

In this report, we describe the synthesis and characterization of chiral iridium(III) complexes containing *R*-(+)-BINAP (*R*)-(+)-2,2′-bis(diphenylphosphino)-1,1′-binaphthyl), including two salts of the same cation, [Ir(CO)(Me)(DIM)(*R*)-(+)-BINAP)][SbF_6]$_2$ (**5**) and [Ir(CO)(Me)(DIM)(*R*)-(+)-BINAP)]-[BAr_4^f]$_2$ (**6**) (DIM = diethyl *iso*-propylidenemalonate), and a study of their catalytic properties. In addition to catalyzing the Nazarov cyclization, the Ir(III) salts **5** and **6** are found to catalyze spirocycle formation as shown in Scheme 1 in the presence of specific additives in the reaction solutions.

Results and Discussion

Synthesis and Characterization of IrI_2(CO)(Me)(*R*)-(+)-BINAP). According to the reported procedure,[15] reaction of (n-Bu_4N)[$Ir(CO)_2I_2$] with (*R*)-(+)-BINAP (*R*)-(+)-2,2′-bis(diphenylphosphino)-1,1′-binaphthyl) in toluene results in the formation of IrI(CO)((*R*)-(+)-BINAP) (**3**) in 85% yield. Because of the chiral nature of (*R*)-(+)-BINAP ligand, oxidative addition of MeI to **3** gives two diastereomers of IrI_2(CO)(Me)((*R*)-(+)-BINAP), denoted **4a** and **4b**, that differ in the chirality at the metal center following trans oxidative addition to yield a product with two iodides cis to each other, as well as the BINAP chelate with cis P donors. When 10 equiv of MeI are used, as described for synthesis of IrI_2(CO)(Me)(dppe),[16] the reaction proceeds very slowly, and leads to only 25% conversion after 12 h at room temperature. $^{31}P\{^1H\}$ NMR spectroscopy of the reaction mixture shows the formation of the two diastereomers **4a** and **4b** at early stages of the reaction, but significant decomposition occurs before the reaction is complete. This observation is in contrast to the reported syntheses of analogous complexes IrI_2(CO)-(Me)(dppe)[16] and IrI_2(CO)(Me)(duphos) (duphos = 1, 2-bis-(2,5-di-*iso*-propyl-phospholano)benzene).[17] In both cases, the reaction was complete in several hours. However, for the oxidative addition of MeI to **3**, it was found that using MeI as the solvent results in complete reaction within 3 h, giving **4a** and **4b** in 85% yield with a product ratio of 2:1 (eq 1). A similar ratio of **4a**/**4b** is observed during early stages of the reaction (0.5 h). In the $^{31}P\{^1H\}$ NMR spectrum, **4a** exhibits a pair of doublets at δ −25.6 and −30.8 ($^2J_{PP}$ = 21 Hz) while **4b** shows δ −23.0 and −26.6 ($^2J_{PP}$ = 23 Hz).

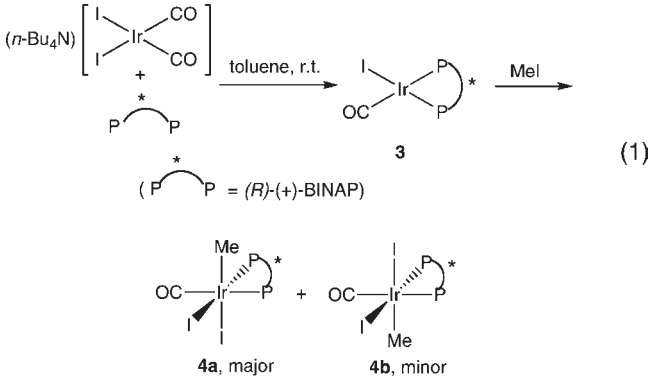

(4) (a) Janka, M.; He, W.; Frontier, A. J.; Eisenberg, R. *J. Am. Chem. Soc.* **2004**, *126*, 6864. (b) Janka, M.; He, W.; Frontier, A. J.; Flaschenreim, C.; Eisenberg, R. *Tetrahedron* **2005**, *61*, 6193.
(5) Janka, M.; He, W.; Frontier, A. J.; Eisenberg, R. *J. Am. Chem. Soc.* **2006**, *128*, 5312–5313.
(6) (a) He, W.; Herrick, I. R.; Atesin, T. A.; Caruana, P. A.; Kellenberger, C. A.; Frontier, A. J. *J. Am. Chem. Soc.* **2008**, *130*, 1003. (b) He, W.; Sun, X.; Frontier, A. J. *J. Am. Chem. Soc.* **2003**, *125*, 14278.
(7) Malona, J. A.; Colbourne, J. M.; Frontier, A. J. *Org. Lett.* **2006**, *8*, 5661.
(8) Bee, C.; Leclerc, E.; Tius, M. A. *Org. Lett.* **2003**, *5*, 4927.
(9) Huang, J.; Frontier, A. J. *J. Am. Chem. Soc.* **2007**, *129*, 8060.
(10) (a) Fujiwara, M.; Kawatsura, M.; Hayase, S.; Nanjo, M.; Itoh, T. *Adv. Syn. Catal.* **2009**, *351*, 123. (b) Kawatsura, M.; Higuchi, Y.; Hayase, S.; Nanjo, M.; Itoh, T. *Synlett*. **2008**, 1009.
(11) Walz, I.; Bertogg, A.; Togni, A. *Eur. J. Org. Chem.* **2007**, 2650.
(12) (a) Liang, G.; Gradl, S. N.; Trauner, D. *Org. Lett.* **2003**, *5*, 4931. (b) Liang, G.; Trauner, D. *J. Am. Chem. Soc.* **2004**, *126*, 9544.
(13) Aggarwal, V. K.; Belfield, A. J. *Org. Lett.* **2003**, *5*, 5075.
(14) Walz, I.; Togni, A. *Chem. Commun.* **2008**, 4315.
(15) Atesin, A. C.; Duckett, S. B.; Flaschenriem, C.; Brennessel, W. W.; Eisenberg, R. *Inorg. Chem.* **2007**, *46*, 1196.
(16) Cleary, B. P.; Eisenberg, R. *Inorg. Chim. Acta* **1995**, *270*, 1970.
(17) Mesfin, J.; Atesin, A. C.; Fox, D. J.; Flaschenriem, C.; Brennessel, W. W.; Eisenberg, R. *Inorg. Chem.* **2006**, *45*, 6559.

Table 1. Crystal Data, Data Collection, and Structure Refinement Parameters for $IrI_2(CO)(Me)((R)\text{-BINAP})$, **4b**, and $[Ir(CO)(Me)(DIM)((R)\text{-BINAP})][SbF_6]_2$, **5**

empirical formula	C51 H47 Cl2 I2 Ir O2 P2	C71.50 H87 Cl F12 Ir O5 P2 Sb2
formula weight	1270.73	1787.50
temperature	100.0(1) K	100.0(1) K
wavelength	0.71073 Å	0.71073 Å
crystal system	orthorhombic	tetragonal
space group	$P2_12_12_1$	$P4_32_12$
unit cell dimensions		
a, Å	12.2235(15)	21.483(2)
b, Å	14.4669(18)	21.483(2)
c, Å	26.899(3)	33.421(7)
volume, Å^3	4756.7(10)	15424(4)
Z	4	8
density (calculated), Mg/m^3	1.774	1.540
absorption coefficient, mm^{-1}	4.324	2.567
F(000)	2464	7120
crystal color, morphology	yellow, block	colorless, block
crystal size, mm^3	0.38 × 0.26 × 0.12	0.24 × 0.18 × 0.10
θ range for data collection	1.60 to 30.51°	1.47 to 32.58°
index ranges	$-17 \le h \le 17$	$-28 \le h \le 32$
	$-20 \le k \le 20$	$-32 \le k \le 32$
	$-38 \le l \le 38$	$-50 \le l \le 50$
reflections collected	74776	208563
independent reflections	14345 [*R*(int) = 0.0434]	28041 [*R*(int) = 0.0918]
observed reflections	12949	22417
absorption correction	multiscan	multiscan
max. and min transmission	0.5950 and 0.2704	0.7833 and 0.5778
data/restraints/parameters	14345/4/515	28041/0/723
goodness-of-fit on F^2	1.039	1.060
final *R* indices [$I > 2\sigma(I)$]	*R*1 = 0.0325, *wR*2 = 0.0780	*R*1 = 0.0561, *wR*2 = 0.1446
R indices (all data)	*R*1 = 0.0382, *wR*2 = 0.0797	*R*1 = 0.0718, *wR*2 = 0.1516

When a higher initial concentration of Ir(CO)I-((*R*)-(+)-BINAP) was employed in the MeI oxidative addition reaction, product precipitation commenced during the course of the reaction. The precipitate contains a mixture of **4a** and **4b** in ratio of 1:19, as determined by its $^{31}P\{^1H\}$ NMR spectrum, while the mother liquor was enriched with **4a** in a ratio of 4:1 to **4b**. Dark orange crystals suitable for X-ray diffraction were obtained by slow diffusion of diethyl ether into a solution of **4b** in dichloromethane at room temperature. Crystallographic data collection and refinement parameters are shown in Table 1, and complete structural details may be found in the CIF supplied in the Supporting Information. A POV-Ray drawing of the structure of **4b** is shown in Figure 1 with selected bond distances and angles given in Table 2.

The crystal structure of **4b** confirms the geometry around the Ir(III) center as essentially octahedral, with a slight distortion in the axial methyl and iodide ligand positions to give a trans angle of 163.47(13)°. The analogous duphos and dppe complexes,[16,17] on the other hand, have less pronounced deviations from linearity in their respective trans Me−Ir−I angle with values of 178.7(4)° and 171.11(8)°. The two Ir−P bond lengths of 2.4091(12) Å and 2.3169(10) Å are consistent with the trans structural influences of CO and iodide ligands, respectively. Other bond distances in the structure of **4b** are similar to those reported for $IrI_2(CO)(Me)(dppe)$[16] and $IrI_2(CO)(Me)$-(duphos).[17]

Synthesis and Characterization of [Ir(CO)(Me)(DIM)-((*R*)-(+)-BINAP)][SbF_6]$_2$ (5) and [Ir(CO)(Me)(DIM)((*R*)-(+)-BINAP)][BAr_4^f]$_2$ (6). When a mixture of diastereomers of **4a** and **4b** (2:1) is reacted with 2 equiv of $AgSbF_6$ in the presence of excess diethyl isopropylidene malonate (DIM) in dichloromethane, two diastereomers of

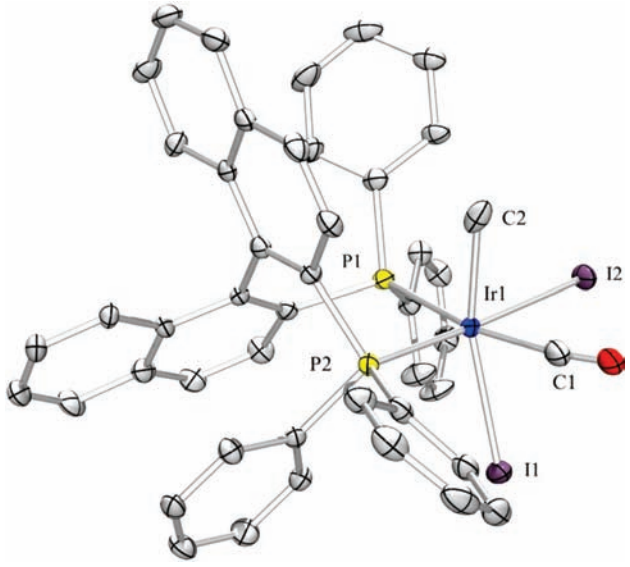

Figure 1. POV-Ray view of **4b** showing the labeling of the atoms around the Ir atom. Displacement ellipsoids are drawn at the 50% level. Hydrogens have been removed for clarity.

Table 2. Selected Bond Lengths (Å) and Angles (deg) of **4b**

Bond Length (Å)			
Ir(1)−P(1)	2.409 (1)	Ir(1)−P(2)	2.317(1)
Ir(1)−C(1)	1.938(6)	Ir(1)−C(2)	2.161(6)
Ir(1)−I(1)	2.8157(5)	Ir(1)−I(2)	2.7390(4)
Bond Angle (deg)			
P(1)−Ir(1)−P(2)	91.20(4)	P(1)−Ir(1)−I(2)	89.38(3)
P(2)−Ir(1)−C(1)	97.1 (2)	C(1)−Ir(1)−I(2)	82.0(2)
C(2)−Ir(1)−I(1)	163.5 (1)	I(1)−Ir(1)−I(2)	88.41(1)
C(1)−Ir(1)−P(1)	170.0 (1)	P(2)−Ir(1)−I(2)	176.29(3)
O(1)−C(1)−Ir(1)	170.1(5)		

$[Ir(CO)(Me)(DIM)((R)\text{-}(+)\text{-}BINAP)]^{2+}$ form in a 90% yield with a ratio of 9:1 (eq 2). The $^{31}P\{^1H\}$ NMR spectrum of the SbF_6^- salt of $[Ir(CO)(Me)(DIM)(R)\text{-}(+)\text{-}BINAP)]^{2+}$, denoted as **5**, exhibits two pairs of doublets at δ 3.1 and −11.9 for the major isomer ($^2J_{PP}$ = 6 Hz) and δ 7.3 and −14.0 ($^2J_{PP}$ = 10 Hz) for the minor isomer. The ^1H NMR spectrum of **5** shows four multiplets (integration of one proton each) centered at 4.97, 4.74, 4.60, and 4.31, respectively, corresponding to four inequivalent methylene protons of the DIM ligand.

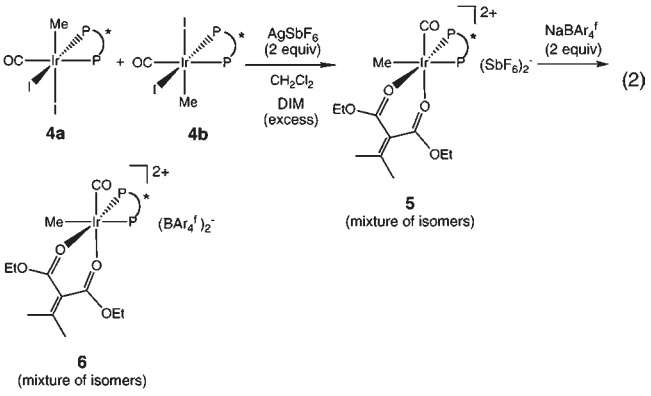

The $(BAr_4^f)^-$ salt ($BAr^f{}_4^- = B(3,5\text{-}(CF_3)_2C_6H_3)_4$) of $[Ir(CO)(Me)(DIM)((R)\text{-}(+)\text{-}BINAP)]^{2+}$ is obtained quantitatively by the reaction of **5** with $NaBAr_4^f$ in dichloromethane (eq 2). This salt is denoted as **6**. The $^{31}P\{^1H\}$ NMR spectrum of **6** shows the same chemical shifts and diastereomeric ratio as those of **5**. The $^{19}F\{^1H\}$ NMR spectrum of **6** also exhibits a singlet peak at δ −63.2, confirming the presence of the BAr_4^{f-} counteranion.

Yellow crystals of one of the diastereomers of **5** suitable for X-ray diffraction were obtained by slow diffusion of hexanes into a concentrated dichloromethane solution of **5** at room temperature. Crystallographic data collection and refinement parameters are shown in Table 1, and complete structural details may be found in the CIF supplied in the Supporting Information. A POV-Ray drawing of the structure of **5** is shown in Figure 2 with selected bond distances and angles given in Table 3.

In the crystal structure of **5**, the iridium(III) center adopts a distorted octahedral coordination geometry, defined by two phosphorus atoms of (*R*)-(+)-BINAP, two oxygen atoms of DIM, a carbonyl, and the methyl ligand. The coordination geometry is necessarily chiral at iridium as a consequence of the two bidentate ligands. The six-membered chelate ring formed by the DIM ligand possesses a boat conformation, which is similar to that observed in the complex $[Cu(S,S\text{-}t\text{-}Bu\text{-}box)\text{-}((MeO_2C)_2C{=}CH(Ph))][SbF_6]_2$[18] and in the dppe analogue of **5**.[4b] The bond distance of Ir(1)−P(1) (2.443(2) Å) is significantly longer than that of Ir(1)−P(2) (2.307(1) Å), consistent with the larger trans structural influence of CO compared to the carbonyl oxygen of DIM. Finally, we note a structural difference between **4b** and **5** in the relative positions of the CO and methyl ligands. In **5** the carbonyl is cis to the two phosphines of the (*R*)-(+)-BINAP ligand, whereas in **4b** the methyl ligand is cis to the two phosphines.

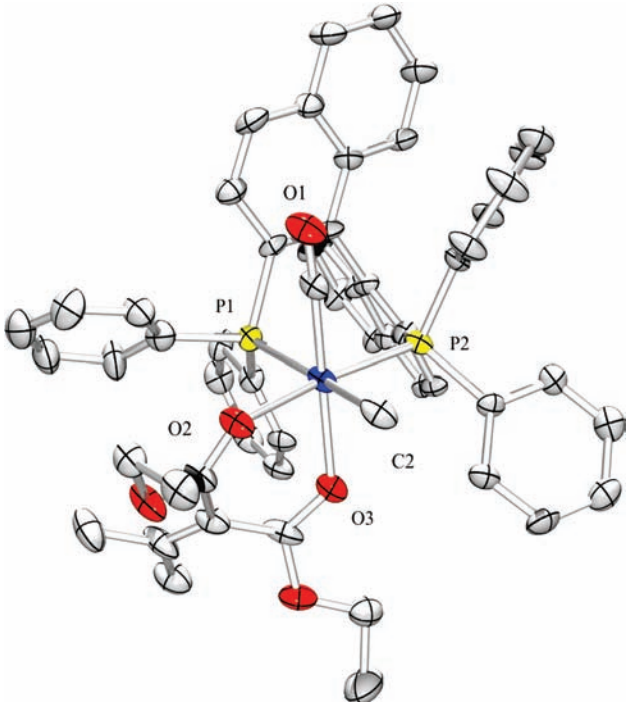

Figure 2. POV-Ray view of **5** showing the labeling of the atoms around the Ir atom. Displacement ellipsoids are drawn at the 50% level. Hydrogens and the anions SbF_6^- have been removed for clarity.

Initial Catalytic Studies of [Ir(CO)(Me)(DIM)((*R*)-(+)-BINAP)]$^{2+}$ in 5 and 6. The electrophilic behavior and catalytic activity of the Ir(III) cation in **5** were examined using previously employed substrates for the Nazarov cyclization and the Diels−Alder reaction. For the Nazarov cyclization, the reaction with substrate **7a** proceeded rapidly (< 5 min at room temperature (rt)) using only 2 mol % of **5** leading to product **7b**, as shown in eq 3. The product was identified by ^1H NMR spectroscopy that showed it to have the same spectrum as that previously reported for **7b** by Frontier *et al.*[6b] This initial success stimulated studies described below with substrates capable of generating quarternary C centers upon Nazarov cyclization.

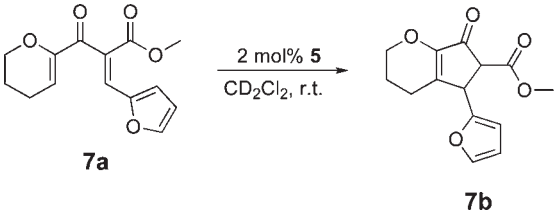

Catalysis of the Diels−Alder reaction was also examined using either isoprene (**8**) or 2,3-dimethylbutadiene (**9**) and methacrolein (**10**) as the dienophile. Both of these reactions proceeded rapidly and were complete in less than 5 min (eqs 4 and 5). The products **11** and **12** were identified by ^1H NMR spectroscopy and comparison of the observed resonances with literature values. However, for the Diels−Alder product obtained with 2,3-dimethylbutadiene, further reaction was observed that is consistent with the

(18) Evans, D. A.; Rovis, T.; Kozlowski, M. C.; Downey, C. W.; Tedrow, J. S. *J. Am. Soc. Chem.* **2000**, *122*, 9134.

Table 3. Selected Bond Lengths (Å) and Angles (deg) of [Ir(CO)(Me)(DIM)(*R*-(+)-BINAP)][SbF_6]$_2$, **5**

Bond Length (Å)			
Ir(1)−P(1)	2.443(2)	Ir(1)−P(2)	2.307(1)
Ir(1)−C(1)	1.861(6)	Ir(1)−C(2)	2.138(7)
Ir(1)−O(2)	2.130(4)	Ir(1)−O(3)	2.125(4)
C(1)−O(1)	1.111(7)		
Bond Angle (deg)			
P(1)−Ir(1)−P(2)	94.14(5)	P(1)−Ir(1)−O(2)	93.0(1)
P(2)−Ir(1)−C(2)	92.1(2)	C(2)−Ir(1)−O(2)	81.0(2)
O(2)−Ir(1)−O(3)	83.6(2)	O(2)−Ir(1)−P(2)	172.6(1)
C(2)−Ir(1)−P(1)	172.2(2)	O(3)−Ir(1)−C(1)	173.6(2)
O(1)−C(1)−Ir(1)	176.8(5)		

significant electrophilicity of the Ir(III) cation [Ir(CO)(Me)(DIM)((*R*)-(+)-BINAP)]$^{2+}$. Specifically, the aldehyde resonance of product **12** was observed to diminish over time and disappeared completely after 5 h at ambient temperature. As that resonance decreased in intensity, three methyl resonances, two singlets, and one doublet were observed to grow in as shown in Figure 3. The identity of the new product was established based on an earlier report by Baldwin and Lusch who observed essentially the same change using $SnCl_4$ as the Lewis acid.[19] The mechanism proposed by Baldwin, which is shown in Scheme 2, yields the bicyclic ketone **13** as the final product and relies on the considerable electrophilicity of the $SnCl_4$ catalyst to promote the rearrangement. The observation of **13** as the final product in the reaction catalyzed by **5** supports the notion of [Ir(CO)(Me)(DIM)((*R*)-(+)-BINAP)]$^{2+}$ as highly electrophilic. The fact that the same rearrangement is not seen when isoprene is used supports the carbocation nature of the rearrangement.

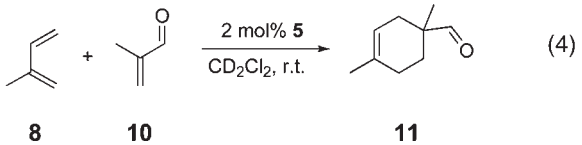

8 **10** **11** (4)

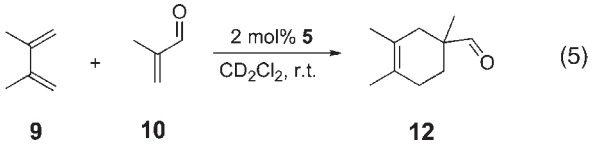

9 **10** **12** (5)

Nazarov Cyclization Catalysis Leading to Quarternary Carbon Generation and Spirocycle Formation. β-Ketoester alkylidene substrates having a methyl substituent at the C1 position were next chosen for Nazarov cyclization and possible spirocycle formation. It was thus found that when a mixture of *E* and *Z* diastereomers of these substrates is treated with catalytic amounts of the Ir(III) catalyst **1**, **5**, or **6** (10% mol), a single diastereomer from Nazarov cyclization is isolated as the product with the configuration corresponding to a conrotatory cyclization of the *Z* isomer. This observation is in agreement with results reported previously using the same substrates in the presence of $Cu(OTf)_2$.[6a] The fact that only a single diastereomeric product forms is consistent

(19) Baldwin, J. E.; Lusch, M. J. *J. Org. Chem.* **1979**, *44*, 1923.

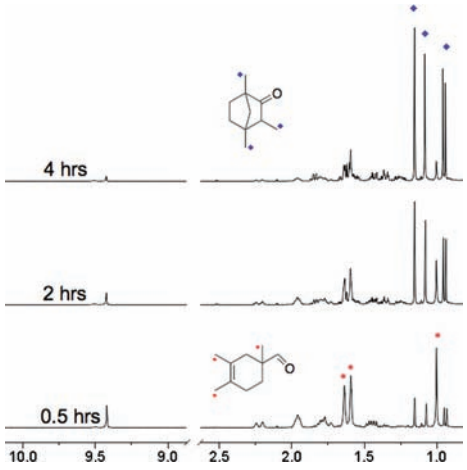

Figure 3. ^{1}H NMR spectra showing the conversion of **12** to **13** overtime in CD_2Cl_2.

Scheme 2

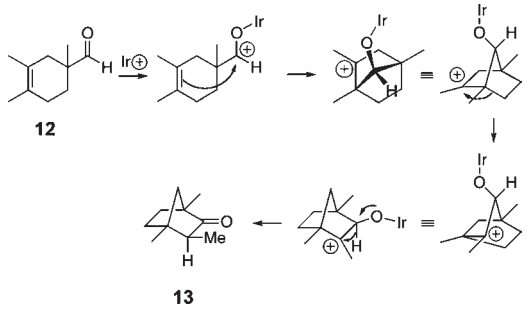

with rapid *E*-*Z* interconversion of the substrate followed by electrocyclization of the *Z* substrate. The results of different runs are summarized in Table 4. It was found that the catalytic activities of **5** and **6** are comparable to that of **1**. In each product, a quarternary center is created at the C1 position upon Nazarov cyclization. As seen previously, cyclization of substrates with aryl substituents at the C5 position (see Table 4 equation for substrate position numbering) occurs more rapidly than with alkyl substituents at that position.

Catalysis of spirocycle formation for the substrate **2a** by the Ir(III) complexes is also seen to occur, as shown in Table 5. For a dilute solution (5 mM) of **2a** in dichloromethane, reaction with 10% mol of the Ir(III) dppe dication **1** yields the Nazarov product **2b** in 48% isolated yield while the spirocycle product **2c** is found to form in only 9% yield. However, when the amount of **1** is increased to stoichiometric (1:1 catalyst:substrate), the spirocycle product **2c** forms in 61% yield while **2b** is obtained in just ~6% yield. In earlier studies by Huang and Frontier,[9] the formation of spirocycle **2c** had been reported in reactions with $Cu(OTf)_2$ and $Cu(SbF_6)_2$ and became selective for the spirocycle product when the Cu(II) salts were present in stoichiometric amounts relative to **2a**. With the Ir(III) salts **5** and **6** as the catalysts, the formation of **2c** also increases with greater amounts of the catalyst, but only leads to a product ratio of **2c**/**2b** of ~ 1:1 ratio when stoichiomeric amounts of **5** or **6** are used.

In previous studies, it had been reported that the addition of simple salts to catalytic Nazarov reactions

Table 4. Nazarov Cyclizations Leading to Quarternary Carbon Formation

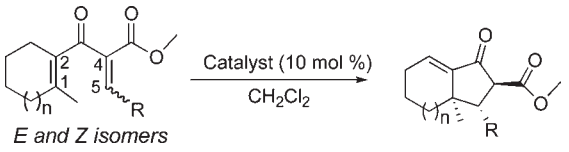

entry	substrate	Ratio *E/Z*	catalyst	time (h)	temp. (°C)	product	yield[a,b] (%)
1	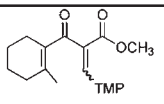 **2a**	40/60	**1**	2	22	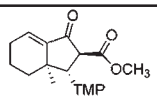 **2b**	48
2	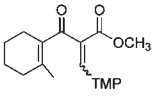 **2a**	40/60	**5**	2	22	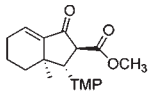 **2b**	62
3	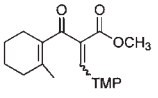 **2a**	40/60	**6**	2	22	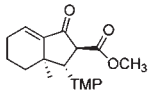 **2b**	51
4	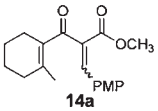 **14a**	62/38	**6**	1	22	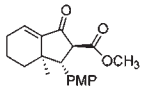 **14b**	75
5	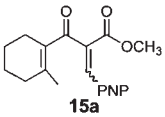 **15a**	95/5	**6**	20	40[c]	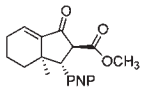 **15b**	81
6	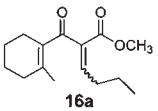 **16a**	51/49	**6**	24	65[c]	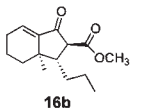 **16b**	55
7	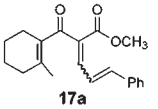 **17a**	57/43	**6**	5.5	22	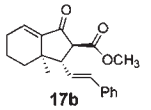 **17b**	85
8	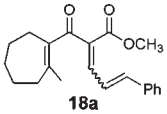 **18a**	51/49	**6**	2	22	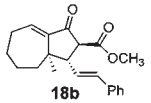 **18b**	90

[a] Reaction conditions: substrate (5 mM) and catalyst (0.5 mM) in dichloromethane. [b] Isolated yield. [c] In 1,2-dichloroethane; TMP = 2,4,6-trimethoxyphenyl; PMP = 4-methoxyphenyl; PNP = 4 -nitrophenyl.

affected the yield and rates of cyclization. For example, stoichiomeric amounts of $LiClO_4$ were found to be essential for efficient cyclization of heteroaryl vinyl ketones with $Sc(OTf)_3$ or $In(OTf)_3$ as the catalyst,[7] and in a recent report, addition of $AgSbF_6$ to solutions containing $[IrBr(CO)((R)\text{-}(+)\text{-BINAP})(DIM)][SbF_6]_2$ as the catalyst, which significantly enhanced that Ir(III) catalyst's activity.[20] Therefore, a study was undertaken to determine the effect of different additives on the relative rates and product distributions of **2c** and **2b** using the Ir(III) complexes **1**, **5**, or **6** as electrophilic catalysts. The results of this study are shown in Table 6.

In contrast with the product ratio obtained in the reaction of **2a** with 10 mol % **1** that yielded 48% **2b** and 9% **2c** (entry 1 in Table 5), when the same reaction is carried out in the presence of 1 equiv of $NaBAr_4^f$ in dichloromethane, spirocycle product **2c** is obtained in 78% yield accompanied by **2b** in 14% yield. Similarly, **2c** is obtained as the major product with catalysts **5** and **6** in 75% and 80% yield, respectively, with **2b** as the minor product in yields of 13% and 12% (Table 6, entries 3 and 6). Control experiments show that Nazarov cyclization of **2a** does not occur with 1 equiv of $NaBAr_4^f$ in the absence of the Ir(III) complex, nor does spirocycle formation take place when the Nazarov product **2b** is treated with $NaBAr_4^f$.

When the amount of $NaBAr_4^f$ is reduced to 0.5 equiv of **2a** and the reaction carried out under the same conditions, the yield of **2c** decreases to 66% while that of **2b** increases to 22% (Table 6, entry 5). Moreover, when 15-crown-5, which is known to complex Na^+, is added to the reaction along with $NaBAr_4^f$, formation of spirocycle **2c** decreases further to a 25% yield while that of the Nazarov product

(20) Vaidya, T.; Atesin, A. C.; Herrick, I. R.; Frontier, A. J.; Eisenberg, R. *Angew. Chemie., Int. Ed.*, in press.

Table 5. Formation of **2b** and **2c** Catalyzed by Ir(III) Complexes **1**, **5**, and **6**

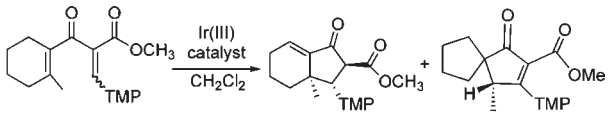

2a (TMP=2,4,6-trimethoxyphenyl) **2b** **2c**

entry	catalyst (mol)	time (h)	temp. (°C)	yield of **2b** (%)/(ee)	yield of **2c** (%)/(ee)	ratio **2b**/**2c**
1	**1** (10%)	4	22	48	9	5.6/1
2	**1** (100%)	4	22	6	61	1/11
3	**5** (10%)	4	22	62	13	4.8/1
4	**5** (100%)	12	22	32	42	1/1.3
5	**6** (10%)	4	22	51 /(15% ee)	7 /(6%ee)	7.9/1
6	**6** (100%)	4	22	17 /(15% ee)	24 /(4%ee)	1/1.4

Table 6. Effects of Additives on Formation of **2b** and **2c** Catalyzed by **6**[a]

entry	catalyst (10 mol %)	additive (mol)	solvent	time (h)	temperature (°C)	yield of **2b** (%)	yield of **2c** (%)	ratio **2b**/**2c**
1	**1**	$NaBAr_4^f$ (100%)	CH_2Cl_2	4	22	13	78	1/6
2	none	$NaBAr_4^f$ (100%)	CH_2Cl_2	6	22	0	0	
3	**5**	$NaBAr_4^f$ (100%)	CH_2Cl_2	4	22	12	75	1/6.3
4	**6**	none	CH_2Cl_2	4	22	51	7	7.9/1
5	**6**	$NaBAr_4^f$ (50%)	CH_2Cl_2	4	22	22	66	1/3
6	**6**	$NaBAr_4^f$ (100%)	CH_2Cl_2	4	22	13 /(7% ee)	80 /(6% ee)	1/6.1
7	**6**	$NaBAr_4^f$ (100%) + 15-crown-5 (100%)	CH_2Cl_2	4	22	72	25	2.9/1
8	**6**	$NaBAr_4^f$ (100%)	CH_3NO_2	4	22	0	0	0
9	**6**	$NaBAr_4^f$ (100%)	CH_2Cl_2 /ether(3/1)	2	22	70	15	4.6/1
10	**6**	$KBAr_4^f$ (100%)	CH_2Cl_2	2.5	22	24 /(8% ee)	75 /(6% ee)	1/3
11	**6**	$ZnCl_2$ (100%)	CH_2Cl_2	1.5	22	16	59	1/3.8
12	**6**	$ZnBr_2$ (100%)	CH_2Cl_2	1.5	22	19 /(8% ee)	74 /(6% ee)	1/3.8
13	**6**	ZnI_2 (100%)	CH_2Cl_2	4	22	6	68	1/11
14	**6**	$Mg(OTf)_2$ (100%)	CH_2Cl_2	1.5	22	77	16	4.9/1
15	**6**	$TlPF_6$ (100%)	CH_2Cl_2	1.5	22	66	15	4.5/1

[a] Reaction conditions catalyst (10 mol %), **2a** (5 mM), catalyst (0.5 mM) and additive (s) (5 mM) in dichloromethane.

2b grows to 72% yield (Table 6, entry 7). These observations support the notion that Na^+ influences the relative selectivity for formation of **2b** and **2c**, which in turn leads to the hypothesis that binding of Na^+ to carbonyl oxygen atoms of **2a** influences positively the formation of **2c**. We hypothesize that by Na^+ coordination, overall carbonyl oxygen basicity is reduced for proton abstraction to complete the Nazarov cyclization sequence, thus favoring the Wagner−Meerwein rearrangement to give **2c**. This notion is further supported by the observation that in solvents containing carbonyl O atoms, the formation of **2c** is not observed (Table 6, entries 8 and 9). Use of $KBAr_4^f$ and ZnX_2 (where X = Cl, Br, I) as additives also leads to predominant formation of **2c** (60−75% yield), whereas addition of $Mg(OTf)_2$ or $TlPF_6$ to the reaction system affords Nazarov product **2b** as the major product (66−77% yield) (Table 6, entries 10 to 15). As with $NaBAr_4^f$, control experiments reveal that none of these additives is found to promote the cyclization of **2a** in the absence of the iridium(III) complexes (**1**, **5**, or **6**).

To determine whether **2b** and **2c** interconvert under the reaction conditions used for their formation, **2b** was dissolved in dichloromethane (5 mM) in the presence of the Ir(III) catalyst **6** (0.5 mM) and $NaBAr_4^f$ (5 mM) at room temperature. However, after 24 h only 5% conversion to **2c** was observed while 95% of **2b** was recovered intact (eq 6). Likewise, when **2c** was dissolved in dichloromethane (5 mM) in the presence of **6** (0.5 mM) and $NaBAr_4^f$ (5 mM) at room temperature, no **2b** was seen after 24 h and **2c** was recovered quantitatively (eq 7). These results indicate that any change in the ratios of Nazarov-to-spirocycle products must occur during the catalytic cycle and not subsequent to product elimination.

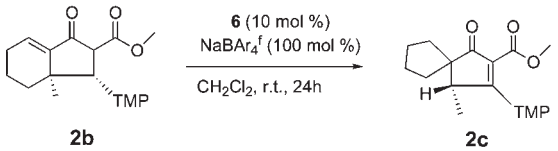

2b **2c** 5 % conversion (6)

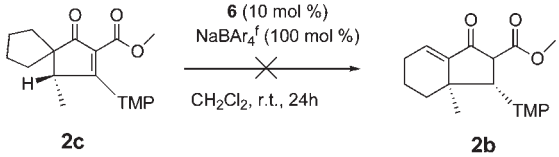

2c **2b** no conversion (7)

The basis of spirocycle formation has been put forward previously[9] and is outlined in Scheme 3. Catalysis of

Scheme 3

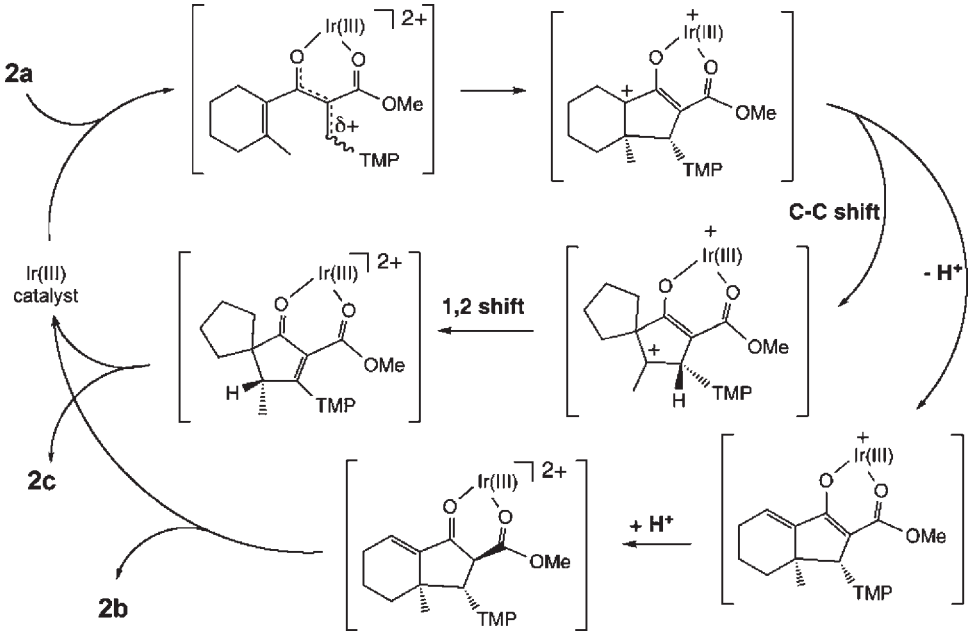

Nazarov cyclization by electrophilic complexes proceeds by initial coordination that activates the substrate to the 4π conrotatory electrocyclization. Once 5-membered ring closure is achieved, the subsequent steps involve proton loss adjacent to the carbocation center and subsequent proton addition elsewhere in the molecule. The branch point to spirocycle formation exists when, following electrocyclization, proton loss is slow or inhibited. Under that condition, a ring contraction can occur yielding a spirocyclic carbocation. The migrating ability of the hydrogen atom (as hydride) or the R substituent on the C atom adjacent to the cationic carbon then determines the specific spirocycle that is produced, following dissociation of the catalyst-product complex.

The observations described above indicate that in catalytic amounts, the Ir(III) cationic complexes are unable to bind to all carbonyl functionality on reactants and products to inhibit facile proton loss so that Nazarov cyclization is the result of the catalysis. However, when the catalyst is present in stoichiometric amounts or other Lewis acids are added to the reaction system to bind all available carbonyl groups on substrates and products, then proton loss from the cyclized Nazarov intermediate is inhibited, at which point Wagner−Meerwein ring contraction to form a more stable intermediate becomes competitive. The use of $NaBAr_4^f$ as an effective additive to the reaction for spirocycle formation takes advantage of the modest but significant Lewis acidity of Na^+ and the non-coordinating and non-basic behavior of the BAr_4^{f-} anion.

A final series of studies regarding spirocycle formation was conducted in which the substituent at the C5 position of the Nazarov substrate was varied to see whether or not it migrated to the substrate C1 position during spirocycle formation. Previously, Huang and Frontier[9] had found that the migration tendency of alkyl, aryl, and cinnamyl substituents at the C5 position differed, with only the aryl group migrating to give a product having two adjacent quarternary centers. In the studies reported here, different alkylidene β-ketoesters with aryl, alkyl, and cinnamyl substitutents at the C5 position were examined using **6** as the catalyst and 1 equiv of $NaBAr_4^f$ (Table 4). For substrate **2a** having a 2,4,6-trimethoxyphenyl substituent, the spirocycle product that forms in 80% yield has the 2,4,6-trimethoxyphenyl (TMP) substituent remaining bound to the C5 carbon. No evidence is seen in this reaction of aryl group migration. However, in the corresponding reaction with substrate **14a** in which the C5 substituent is 4-methoxyphenyl (PMP), the spirocycle formed in 48% yield corresponds to the one in which only the PMP group has migrated. In this case, no evidence is observed in support of the isomeric spirocycle in which hydride migration occurs.

When substrate **15a** or **16a** is heated in 1,2-dichloroethane with 10% mol of **6** and 1 equiv of $NaBAr_4^f$, the only spirocycle product is **15c** or **16c**, respectively, with no evidence of isomeric **15d** or **16d**, respectively. These results are consistent only with a hydride shift from C5 to C1 leading to the spirocycle product in 45% or 60% yield, respectively. Finally, the cinnamyl-containing substrates **17a** and **18a** when reacted with **6** and 1 equiv of $NaBAr_4^f$ yield **17b** and **18b** as the major products in 43% and 35% yields, respectively. With regard to the spirocycle products for these substrates, yields are poor (14% and 13%, respectively), but products **17d** and **18d** indicate that the migration of the cinnamyl group from C5 to C1 occurs. If the reaction with **17a** and **18a** is conducted using **6** but without 1 equiv of $NaBAr_4^f$ as additive, only the Nazarov product is seen (Table 4). The migration tendencies for the C5 substituents in spirocycle formation that are seen in the present study are in full agreement with the previously published work that employed a *stoichiometric* amount of $[Cu(bisoxazoline)](SbF_6)_2$ as the catalyst.[9]

Results Regarding Asymmetric Induction. While the cationic complex $[Ir(CO)(Me)(DIM)((R)\text{-}(+)\text{-}BINAP)]^{2+}$ in **5** and **6** is chiral, the use of either salt to promote the conversion of **2a** to **2b** and **2c** yielded results in which

product enantiomeric excesses were less than 15%. The basis for this poor enantioselectivity is likely unselective binding of the substrate carbonyl oxygen atoms to the two adjacent but inequivalent binding sites at the iridium center, similar to what has been observed previously at lower temperatures by ^{1}H NMR spectroscopy regarding Nazarov substrate binding to complex **1**.[4b] These studies showed that the Nazarov divinyl β-ketoester substrates chelated to the iridium(III) center through the two carbonyl oxygen atoms, and because of the inequivalence of the two Ir binding sites, two substrate-catalyst diastereomers were observed with little preference for one diastereomer over the other (shown as **19** and **20**). This meant that even if the chirality at the Ir(III) center was sufficient to control the direction of conrotation in the Nazarov electrocyclization, unselective substrate binding would lead to poor enantioselectivity.

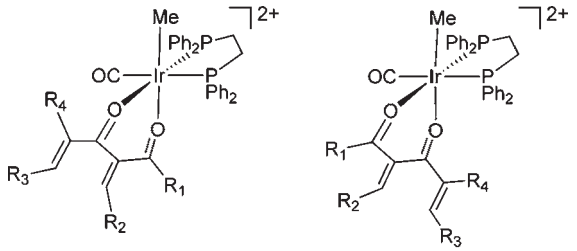

(R$_1$, R$_2$, R$_3$, R$_4$ = alkyl, aryl)

19 **20**

Conclusions

The synthesis and catalytic activity of the new electrophilic dicationic complex [Ir(CO)(Me)(DIM)((*R*)-(+)-BINAP)]$^{2+}$ which has been isolated as its SbF_6^- salt **5** and BAr_4^{f-} salt **6** have been described. The structure of the cationic complex has been confirmed crystallographically, and its strong electrophilic nature coupled with the weak binding ability of diethyl isopropylidenemalonate makes the iridium(III) center of **5** or **6** a strong Lewis acid catalyst for polarized Nazarov cyclizations and the Diels−Alder cycloaddition reaction. A carbocation rearrangement of the Diels−Alder product formed between methacrolein and 2,3-dimethylbutadiene that has previously been reported supports the notion of the high degree of Lewis acidity for the Ir(III) cation [Ir(CO)(Me)(DIM)((*R*)-(+)-BINAP)]$^{2+}$. Catalysis of the Nazarov cyclization using **5** or **6** with substrates capable of generating a quarternary center upon ring closure proceeds readily along with minor amounts of a spirocyclic product. However, through the addition of metal salts to the reaction solutions, the ratio of Nazarov to spirocycle products are found to be adjustable with a stoichiometric amount of $NaBAr_4^f$ being particularly effective in biasing the system to spirocycle formation.

Experimental Section

General Methods. Unless otherwise stated, all the reactions and manipulations were performed in oven-dried glassware under purified nitrogen atmosphere using either standard Schlenk techniques or an inert-atmosphere glovebox. [*n*-Bu$_4$N][Ir(CO)$_2$I$_2$],[16] [IrMe(CO)(dppe)(DIB)](BAr$_4^f$)$_2$,[2] Ir(CO)I(*R*)-(+)-BINAP),[15] NaBAr$_4^f$,[21] and KBAr$_4^f$ [22] were synthesized according to the published procedures. Known Nazarov substrates (**2a**, **7a**, **14a**−**18a**) were prepared and characterized as reported before.[6a,9] All solvents (dichloromethane, tetrahydrofuran (THF), toluene, hexanes, and diethyl ether) were purified and dried under nitrogen by conventional methods.[23] Dichloromethane-d_2 and benzene-d_6 were purchased from Cambridge Isotope Laboratories, degassed and stored in a dry glovebox prior to use. ^{1}H NMR, ^{31}P{^{1}H} NMR, and ^{13}C{^{1}H} NMR spectra were recorded on either a Bruker Avance 400 MHz or a Bruker Avance 500 MHz spectrometer. ^{1}H and ^{13}C{^{1}H} chemical shifts are reported in parts per million after referencing to the appropriate solvent resonances. ^{31}P{^{1}H} chemical shifts are reported relative to an external 85% solution of phosphoric acid. Elemental analyses were done at Quantitatives Technologies Inc. (QTI) or Desert Analystic Inc. X-ray crystal structures were obtained using a Bruker SMART APEX II CCD Platform diffractometer, solved using SIR97, and refined with SHELXL-97.

Synthesis of IrI$_2$(CO)(Me)((*R*)-(+)-BINAP), 4. The complex Ir(CO)I((R)-(+)-BINAP) (100 mg, 0.103 mmol) was dissolved in MeI (10 mL) and the solution was stirred at room temperature for 3 h. The color of the solution turned from dark red to yellow. After removal of the solvent to half its amount (5 mL), diethyl ether (20 mL) was added slowly to precipitate a yellow solid, which was filtered, washed with diethyl ether (3 × 1.5 mL), and dried under vacuum. A mixture of **4a** and **4b** was obtained (0.098 g, 85% yield). The ^{31}P{^{1}H} NMR spectrum of the yellow solid in CD_2Cl_2 shows the presence of **4a** and **4b** in a ratio of 2:1. Anal. Calcd for $C_{46}H_{35}I_2IrOP_2$: C, 49.70, H, 3.17. Found: C, 50.01, H, 3.05.

4a: ^{1}H NMR (CD_2Cl_2, ppm): δ 8.50−6.00 (32 H, m, overlapping naphthyl and aryl H), 2.15 (dd, 3H, J_{PH} = 3.5 Hz, 5.4 Hz, CH_3); ^{31}P{^{1}H} (CD_2Cl_2, ppm): δ −25.59 (d, J_{PP} = 20.9 Hz, 1P), −30.78 (d, J_{PP} = 20.9 Hz, 1P).

4b: ^{1}H NMR (CD_2Cl_2, ppm): δ 8.50−6.00 (32 H, m, overlapping naphthyl and aryl H), 1.24 (dd, 3H, J_{PH} = 4.3 Hz, 6.0 Hz, CH_3); ^{31}P{^{1}H} (CD_2Cl_2, ppm): δ −23.01 (d, J_{PP} = 23.5 Hz, 1P), −26.56 (d, J_{PP} = 23.5 Hz, 1P).

Synthesis of [Ir(CO)(Me)(DIM)((R)-(+)-BINAP)][SbF$_6$]$_2$, 5. Into an oven-dried round-bottom flask was placed a mixture of diastereomers **4a** and **4b** (in a 2:1 ratio) (100 mg, 0.090 mmol), and DIM (90 μL, 0.45 mmol) in CH_2Cl_2 (50 mL). $AgSbF_6$ was then added to the rapidly stirred solution followed by 5 mL of CH_2Cl_2. After 5 min of stirring in the dark, the resulting AgI precipitate was removed by filtration, and the yellow filtrate was concentrated under vacuum to about 5 mL. Diethyl ether (20 mL) was then added slowly to yield a yellow solid. This yellow solid was filtered and washed with diethyl ether (3 × 1.5 mL). A mixture of two diastereomers of **5** was obtained (0.098 g, 85% yield) in a ratio of 9:1 as determined by ^{31}P{^{1}H} NMR spectroscopy. Anal. Calcd for $C_{56}H_{51}F_{12}IrO_6P_2Sb_2$: C, 43.97, H, 3.36. Found: C, 43.83, H, 3.30.

Major Isomer. ^{1}H NMR (CD_2Cl_2, ppm): δ 8.20−6.10 (32H, m, overlapping naphthyl and aryl H), 4.97 (m, 1H, CH_3-CH_2O), 4.74 (m, 1H, CH_3-CH_2O), 4.60 (m, 1H, CH_3-CH_2O), 4.31 (m, 1H, CH_3-CH_2O), 2.33 (s, 3H, $CH_3(CH_3)C=$), 2.02 (s, 3H, $CH_3(CH_3)C=$), 1.55 (t, J_{HH} = 7.5 Hz, CH_3-CH_2O), 1.35 (t, 3H, J_{HH} = 7.5 Hz, CH_3-CH_2O), 1.01 (dd, 3H, J_{PH} = 3.5 Hz, 5.4 Hz, CH_3); ^{31}P{^{1}H} (CD_2Cl_2, ppm): δ 3.10 (d, J_{PP} = 6.3 Hz, 1P), −11.92 (d, J_{PP} = 6.3 Hz, 1P).

Minor Isomer. ^{1}H NMR (CD_2Cl_2, ppm): All the signals were overlapped with major isomer which could not be identified. ^{31}P {^{1}H} (CD_2Cl_2, ppm): δ 7.34 (d, J_{PP} = 10.1 Hz, 1P), −14.04 (d, J_{PP} = 10.1 Hz, 1P).

Synthesis of [Ir(CO)(Me)(DIM)((R)-(+)-BINAP)][BAr$_4^f$]$_2$, 6. To an oven-dried round-bottom flask was added complex **5** (126 mg, 0.082 mmol) in CH_2Cl_2 (20 mL). $NaBAr_4^f$ (153 mg,

(21) Yakelis, N. A.; Bergman, R. G. *Organometallics* **2005**, *24*, 3579.
(22) Buschmann, W. E.; Miller, J. S. *Inorg. Synth.* **2002**, *33*, 83.
(23) Pangborn, A. B.; Giardello, M. A.; Grubbs, R. G.; Timmers, F. J. *Organometallics* **1996**, *15*, 1518.

0.173 mmol) was then added to the rapidly stirred solution followed by 2 mL of CH_2Cl_2. After stirring at room temperature for 1 h, the mixture was filtered, and the yellow filtrate was concentrated under vacuum to about 4 mL. Hexanes (20 mL) were then added slowly. The yellow oil thus formed was decanted from the solvent, dissolved in CH_2Cl_2 (2 mL), and filtered through a pad of Celite to remove small amounts of $NaSbF_6$. Upon addition of hexanes (10 mL) to the filtrate, a yellow oil formed, which was separated from the solvent and stirred in hexanes (10 mL) to yield a yellow solid, that was filtered, washed with hexanes (3 × 1 mL), and dried under vacuum for several hours. The yellow solid **6** was obtained in 220 mg (97%). The $^{31}P\{^1H\}$ NMR spectrum of **6** shows the same signals as did **5** with the same ratio of the isomers. The $^{19}F\{^1H\}$ NMR spectrum of **6** shows a strong signal of δ at −63.2 corresponding to the BAr_4^f anion. This complex was used directly without further characterization.

General Procedures for Catalytic Reactions Involving Ir(III) Complexes 1, 5, and 6. (a) In a glovebox, a J-Young tube was charged with catalyst complex **1**, **5**, or **6** (0.005 mmol) and the particular substrate (0.05 mmol) in CD_2Cl_2 (0.7 mL) and was sealed with a Teflon cap. The J-Young tube was then brought to the desired temperature, and the ensuing reaction was monitored by ^1H NMR spectroscopy. Each experiment was repeated two times. The product was purified by flash column chromatography on silica gel and confirmed by its ^1H NMR spectrum relative to that reported previously for known Nazarov cyclization products.

(b) In a glovebox, a dried 20 mL vial was charged with **6** (0.005 mmol), a substrate (0.05 mmol), and an additive (0.05 mmol) if examined (Table 6) in CH_2Cl_2 (10 mL) or 1, 2-dichloroethane and sealed with a Teflon cap. The solution was stirred at room temperature or higher for several hours (shown in Table 6), and the ensuing reaction was monitored by thin layer chromatography. After the substrate was consumed, the solution was taken to dryness and the residue was passed through a small silica gel column to remove the metal complex. The organic products were collected and confirmed by their ^1H NMR data as compared to reported known samples. The yields of the Nazarov products were estimated by comparison of their ^1H NMR resonances using mesitylene (10 μL) as an internal standard. Each experiment was repeated two times.

(c) In a glovebox, a dried 20 mL vial was charged with **6** (0.005 mmol), substrate **2c** (0.05 mmol), and $NaBAr_4^f$ (0.05 mmol) in CH_2Cl_2 (10 mL) and sealed with a Teflon cap. The solution was stirred at room temperature for 24 h, and the resulting solution was monitored by thin layer chromatography. No **2b** was seen to form after 24 h.

(d) In a glovebox, a dried 20 mL vial was charged with **6** (0.005 mmol), substrate **2b** (0.05 mmol), and $NaBAr_4^f$ (0.05 mmol) in CH_2Cl_2 (10 mL) and sealed with a Teflon cap. The solution was stirred at room temperature for 24 h, and the resulting solution was monitored by thin layer chromatography. The solution was then taken to dryness, and the residue was passed through a small silica gel column to remove any metal complexes. The organic products were collected and confirmed by their ^1H NMR data as compared to reported samples. The yield of the **2c** (5%) was obtained by comparing its ^1H NMR resonances against mesitylene (10 μL) as an internal standard. Each experiment was repeated twice.

(e) In a glovebox, a dried 20 mL vial was charged with a substrate (0.05 mmol) and an additive (0.05 mmol) in CH_2Cl_2 (10 mL) or 1,2-dichloroethane and sealed with a Teflon cap. The solution was stirred at room temperature or higher for a specified time (the reaction conditions are the same as the entries in Table 6, but without the catalyst), and the resulting reaction was monitored by thin layer chromatography. Neither Nazarov cyclization product nor spirocycle product was observed to form in these control reactions.

^1H NMR and MS data are given below for the different products detected in the catalytic reactions. All of these compounds, except for **15c**, have been reported previously in the literature, and references to their initial reports are cited.

Methyl 5-(2-furyl)-7-oxo-2,3,4,5,6,7-hexahydrocyclopenta-[*b*]-pyran-6-carboxylate (7*b*).[6b] ^1H NMR(400 MHz, $CDCl_3$) δ 1.94 (m, 2H), 2.19 (m, 1H), 2.27 (m, 1H), 3.52 (d, J = 2 Hz, 1H, 3.76 (s, 3H), 4.13 (m, 2H), 4.35 (d, J = 2 Hz, 1H), 6.17 (d, J = 3.2 Hz, 1H), 6.31 (t, J = 1.2 Hz, 1H), 7.33 (d, J = 1.2 Hz, 1H); $^{13}C\{^1H\}$ ($CDCl_3$, 100 MHz) δ 21.1, 22.2, 40.8, 52.8, 55.6, 66.9, 107.2, 110.3, 142.4, 144.7, 149.4, 151.7, 168.4, 192.0. Elemental Analysis Calcd. for $C_{14}H_{14}O_5$: C, 64.12%, H, 5.38%; Found: C, 64.00%, H, 5.51%.

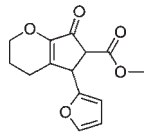

7b

1,4-Dimethyl-3-cyclohexene-1-carboxaldehyde (11).[24] ^1H NMR (CD_2Cl_2, ppm): δ 9.51 (s, 1H), 5.45 (m, 1H), 2.44−2.30 (m, 1H), 2.08−1.98 (m, 2H), 1.96−1.81 (m, 2H), 1.52 (bs, 3H), 1.57 (m, 1H), 1.09 (s, 3H); MS (e/z) 138.11.

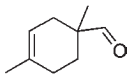

11

1,3,4-Trimethyl-3-cyclohexene-1-carbaldehyde (12).[25] ^1H NMR (CD_2Cl_2, ppm): δ 9.42 (s, 1H), 2.28−2.18 (m, 1H), 2.00−1.93 (m, 2H), 1.76 (m, 2H), 1.64 (bs, 3H), 1.60 (bs, 3H), 1.44 (m, 1H), 1.00 (s, 3H); MS (e/z) 152.13.

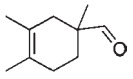

12

1,3-*exo*-4-Trimethylbicyclo[2.2.l]heptan-2-one (13).[19] ^1H NMR (CD_2Cl_2, ppm): δ 1.84 (q, 1H, J = 7.1 Hz), 1.67−1.54 (m, 1H), 1.46−1.38 (m, 2H), 1.37−1.32 (m, 2H), 1.31−1.24 (m, 1H), 1.15 (s, 3H), 1.10 (s, 3H), 0.96 (d, 3H, J = 7.2 Hz); MS (e/z) 152.12.

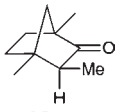

13

Methyl 3a-Methyl-1-oxo-3-(2,4,6-trimethoxyl-phenyl)-2,3,3a, 4,5,6-hexahydro-1*H*-indene-2-carboxylate Ester (2b).[6b] ^1H NMR (400 MHz, $CDCl_3$): δ 6.74 (t, J = 4 Hz, 1H), 6.15 (s, 2H), 4.90 (d, J = 13.2 Hz, 1H), 4.05 (d, J = 13.2 Hz, 1H), 3.81 (s, 3H), 3.77 (s, 6H), 3.66 (s, 3H), 2.21 (m, 2H), 1.63−1.71 (m, 4H), 1.24 (s, 3H), $^{13}C\{^1H\}$ ($CDCl_3$, 100 MHz): δ 200.0, 170.6, 159.9, 144.8, 134.4, 105.9, 91.5, 55.1, 52.1, 45.6, 41.9, 34.1, 25.5, 20.6, 18.1.

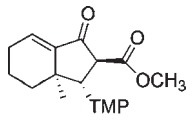

2b

Methyl 3-(4-Methoxy-phenyl)-3a-methyl-1-oxo-2,3,3a4,5,6-hexahydro-1*H*-indene-2-carboxylate (14b).[6a] ^1H NMR (400 MHz, $CDCl_3$): δ 0.80 (s, 3 H), 1.51 (m, 1 H), 1.67 (m, 1 H),

(24) Roberston, J.; Fowler, T. G. *Org. Biomol. Chem.* **2006**, *4*, 4307.
(25) Teo, Y.; Loh, T. *Org. Lett.* **2005**, *7*, 2539.

1.85 (m, 2 H), 2.29 (m, 1 H), 2.35 (m, 1H), 3.44 (d, 1H, J = 13.1 Hz), 3.70 (s, 3H), 3.82 (s, 3H), 3.92 (d, 1H, J = 13.1 Hz), 6.84 (t, 1H, J = 3.6 Hz), 6.90 (d, 2H, J = 8.8 Hz), 7.18 (d, 2H, J = 8.8 Hz); $^{13}C\{^1H\}$ NMR (100 MHz, $CDCl_3$): δ 17.9, 20.3, 25.4, 34.5, 40.6, 52.4, 54.9, 55.2, 56.2, 113.7, 128.2, 129.1, 135.4, 144.5, 158.7, 169.8, 197.8; HRMS calculated for $C_{19}H_{22}O_4$ $(M+H)^+$: 315.1591, Found: 315.1594.

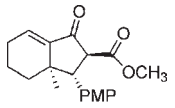

14b

Methyl 3-(4-Nitrophenyl)-3a-methyl-1-oxo-2,3,3a,4,5,6-hexahydro-1*H*-indene-2-carboxylate (15b).[6a] ^1H NMR (400 MHz, $CDCl_3$): δ 0.81 (s, 3 H), 1.69 (m, 4 H), 2.31 (m, 2 H), 3.60 (d, 1H, J = 12.8 Hz), 3.71 (s, 3H), 3.98 (d, 1H, J = 12.8 Hz), 6.88 (t, 1H, J = 3.6 Hz), 7.43 (d, 2H, J = 8.8 Hz), 8.22 (d, 2H, J = 8.8 Hz); $^{13}C\{^1H\}$ NMR (100 MHz, $CDCl_3$): δ 17.9, 20.6, 25.4, 34.6, 40.9, 52.8, 55.4, 55.8, 123.7, 129.0, 136.6, 143.5, 144.3, 147.3, 169.1, 196.6; HRMS calculated for $C_{18}H_{20}NO_5$ $(M+H)^+$: 330.1341, Found: 330.1337.

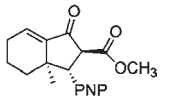

15b

Methyl 3a-Methyl-1-oxo-3-propyl-2,3,3a,4,5,6-hexahydro-1*H*-indene-2-carboxylate (16b).[6a] ^1H NMR (400 MHz, $CDCl_3$): δ 0.94 (t, 3H, J = 7.2 Hz), 0.99 (s, 3H), 1.33 (m, 2H), 1.35 (m, 2H), 1.45 (m, 1H), 1.79 (m, 2H), 1.98 (m, 1H), 2.21 (m, 2H), 2.31 (m, 1H), 3.15 (d, 1H, J = 11.9 Hz), 3.77 (s, 3H), 6.70 (t, 1H, J = 3.6 Hz); $^{13}C\{^1H\}$ NMR (100 MHz, $CDCl_3$): δ 14.4, 18.1, 19.7, 21.4, 25.3, 32.1, 34.8, 39.2, 50.0, 58.8, 134.2, 145.2, 171.1, 199.5; HRMS calculated for $C_{15}H_{22}O_3$ $(M+Na)^+$: 273.1461, Found: 273.1463.

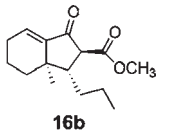

16b

Methyl 3a-Methyl-1-oxo-3-styryl-2,3,3a,4,5,6-hexahydro-1*H*-indene-2-carboxylate (17b).[6a] ^1H NMR (400 MHz, $CDCl_3$): δ 1.08 (s, 3 H), 1.37 (m, 1H), 1.82 (m, 2H), 1.97 (m, 2H), 2.36 (m, 2H), 2.99 (dd, 1H, J_1 = 12.2 Hz, J_2 = 8.0 Hz), 3.56 (d, 1H, J = 12.2 Hz), 3.77 (s, 3H), 6.24 (dd, 1H, J_1 = 15.8 Hz, J = 8.0 Hz), 6.54 (d, 1H, J = 15.8 Hz), 6.80 (t, 1H, J = 3.6 Hz), 7.27 (d, 2H, J = 6.5 Hz), 7.35 (d, 2H, J = 6.5 Hz); $^{13}C\{^1H\}$ NMR (100 MHz, $CDCl_3$): δ 17.8, 20.5, 25.3, 34.3, 40.3, 52.3, 53.8, 57.2, 125.7, 126.2, 127.5, 128.4, 133.0, 135.1, 136.1, 144.2, 169.7, 198.0; HRMS calculated for $C_{20}H_{22}O_3$ $(M+H)^+$: 311.1642, Found: 311.1632.

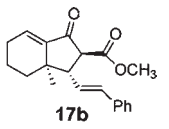

17b

Methyl 3a-Methyl-1-oxo-3-styryl-1,2,3,3a,4,5,6,7-octahydroazulene-2-carboxylic Methyl Ester (18b).[6a] ^1H NMR (400 MHz, $CDCl_3$): δ 1.13 (s, 3 H), 1.47 (m, 4H), 1.98 (m, 2H), 2.30 (m, 1 H), 2.51 (m, 1H), 3.45 (dd, 1H, J_1 = 8.6 Hz, J_2 = 8.6 Hz), 3.55 (d, 1H, J = 16.1 Hz), 3.75 (s, 3H), 6.18 (dd, 1H, J_1 = 8.6 Hz, J = 8.6 Hz), 6.55 (d, 1H, J = 15.7 Hz), 7.02 (t, 1H, J = 3.6 Hz), 7.33 (m, 5H); $^{13}C\{^1H\}$ NMR (100 MHz, $CDCl_3$): δ 18.6, 24.8, 27.3, 28.3, 38.4, 45.9, 52.3, 52.8, 58.0, 125.4, 126.2, 127.5, 128.4, 133.9, 136.6, 139.8, 146.5, 169.7, 198.0; HRMS calculated for $C_{21}H_{24}O_3$ $(M+H)^+$: 325.1798, Found: 325.1799.

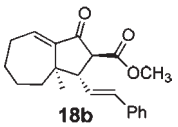

18b

Methyl 4-Methyl-1-oxo-3-(2,4,6-trimethoxy)phenylspiro[4,4]non-2-ene-2-carboxylate (2c).[9] ^1H NMR (400 MHz, $CDCl_3$) δ: 0.89 (d, 3H, J = 7.2 Hz), 1.64−1.68 (m, 4H), 1.67−1.86 (m, 4H), 3.29 (q, 1H, J = 7.2 Hz), 3.65 (s, 3H), 3.72 (s, 6H), 3.82 (s, 3H), 6.12 (s, 2H); $^{13}C\{^1H\}$ NMR (100 MHz, $CDCl_3$) (ppm): δ 15.99, 25.33, 25.39, 30.72, 40.17, 48.25, 51.39, 55.33, 55.63, 59.56, 90.64, 105.64, 131.89, 157.87, 162.48, 164.25, 178.48, 207.94; HRMS (ESI) for $[C_{21}H_{27}O_6]+$ Calcd: 375.1802, Found: 375.1802.

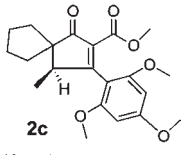

2c

Methyl 4-(4-Methoxyphenyl)-4-methyl-1-oxo-spiro[4,4]non-2-ene-2-carboxylate (14d).[9] ^1H NMR (400 MHz, $CDCl_3$): δ 0.87 (m, 1H), 1.23 (m, 1H), 1.34 (m, 1H), 1.47 (s, 3H), 1.57 (m, 2H), 1.75 (m, 1H), 1.85 (m, 1H), 1.95 (m,1H), 3.78 (s, 3H), 3.85 (s, 3H), 6.85 (d, 2H, J = 7.2 Hz), 7.06 (d, 2H, J = 7.2 Hz), 8.37 (s, 1H); $^{13}C\{^1H\}$ NMR (100 MHz, $CDCl_3$) δ (ppm): 24.29, 25.00, 25.22, 30.89, 36.08, 51.65, 52.09, 55.26, 66.15, 113.88, 128.20, 132.65, 134.00, 158.61, 162.86, 175.85, 207.10; HRMS (ESI) for $[C_{19}H_{23}O_4]^+$ Calcd. 315.1591, Found 375.1589.

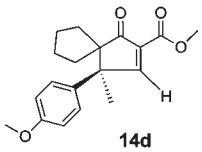

14d

Methyl 4-Methyl-3-(4-nitrophenyl)spiro[4,4]non-2-ene-2-carboxylate (15c). ^1H NMR (400 MHz, CD_2Cl_2): δ 1.00 (d, 3H, J_{HH} = 7.2 Hz), 1.69−1.78 (m, 4H), 1.86−1.96 (m, 4H), 3.14 (q, 1H, J_{HH} = 7.2 Hz), 3.66 (s, 3H), 7.56 (d, 2H, J_{HH} = 8.8 Hz), 8.29 (d, 2H, J_{HH} = 8.8 Hz); $^{13}C\{^1H\}$ NMR (100 MHz, CD_2Cl_2) (ppm): δ 16.3, 25.46, 30.05, 30.91, 41.00, 49.29, 52.46, 60.28, 124.09, 128.67, 133.40, 141.13, 148.89, 164.31, 175.95, 207.00; IR(thin film): 2960, 1739, 1728, 1596, 1521, 1347, 1270; HRMS calculated for $C_{18}H_{20}NO_5$ $(M+H)^+$: 330.1341, Found: 300.1330:

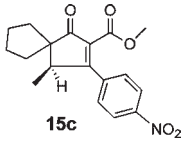

15c

Methyl 4-Methyl-1-oxo-3-propylspiro[4,4]non-2-ene-2-carboxylate (16c).[9] ^1H NMR (400 MHz, $CDCl_3$) δ (ppm): 0.97 (t, 3H, J = 7.5 Hz), 1.09 (d, 3H, J = 7.5 Hz), 1.39−1.44 (m, 1H), 1.45−1.55 (m, 1H), 1.54−1.64 (m, 4H), 1.78−1.86 (m, 4H), 2.40−2.44 (m, 1H), 2.61 (q, 1H, J = 7.2 Hz), 2.97−3.00 (m, 1H), 3.82 (s, 3H); $^{13}C\{^1H\}$ NMR (100 MHz, $CDCl_3$) (ppm): δ 14.22, 15.83, 21.14, 25.05, 25.25, 30.22, 31.89, 40.45, 48.12, 51.74, 59.52, 129.89, 164.24,

189.76, 207.41; HRMS (ESI) for $[C_{15}H_{23}O_3]^+$ Calcd: 251.1642, Found: 251.1644.

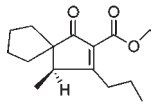

16c

Methyl 4-Methyl-1-oxo-4-[(*E*)-2-phenylvinyl]spiro[4,4]non-2-ene-2-carboxylate (17d).[9] ^{1}HNMR (400 MHz, $CDCl_3$) (ppm): δ 1.32 (s, 3H), 1.50−1.86 (m, 8H), 3.85 (s, 3H), 6.01 (d, 1H, J = 16.0 Hz), 6.31 (d, 1H, J = 16.0 Hz), 7.28−7.34 (m, 5H), 8.19 (s, 1H). ^{13}C {^{1}H}NMR (100 MHz, $CDCl_3$): δ: 22.70, 24.67, 24.94, 32.18, 34.39, 50.41, 52.05, 65.49, 126.24, 127.86, 128.65, 130.28, 132.07, 133.03, 136.44, 162.72, 174.57, 206.31; HRMS (ESI) for $[C_{20}H_{23}O_3]^+$ Calcd: 311.1642, Found: 311.1648.

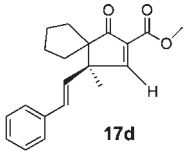

17d

Methyl 4-Methyl-1-oxo-4-[(*E*)-2-phenylvinyl]spiro[4,5]dec-2-ene-2-carboxylate (18d).[9] ^{1}H NMR (400 MHz, $CDCl_3$) δ (ppm): 1.20−1.95 (m, 10 H), 1.31 (s, 3H), 3.87 (s, 3H), 6.09 (d, 1H, J = 16.0 Hz), 6.24 (d, 1H, J = 16.0 Hz), 7.31−7.33 (m, 5H), 8.12 (s, 1H); ^{13}C{^{1}H} NMR (100 MHz, $CDCl_3$) (ppm): δ 22.05, 22.11, 22.57, 25.58, 30.20, 32.67, 51.78, 52.07, 56.83, 126.27, 127.86, 128.70, 129.00, 130.10, 132.47, 136.54, 162.87, 173.55, 206.43; HRMS (ESI) for $[C_{21}H_{25}O_3]^+$ Calcd: 325.1798, Found: 325.1794.

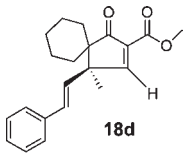

18d

Crystal Structure Determinations. Each crystal was placed onto the tip of a glass fiber and mounted on a Bruker SMART Platform diffractometer equipped with an APEX II CCD area detector. All data were collected at 100.0(1) K using MoKα radiation (graphite monochromator).[26] Data collections were carried out with frame exposure times of 20 (**4b**) and 60 (**5**) seconds at a detector distance of 5 cm. Randomly oriented regions of reciprocal space were surveyed for each sample: four major sections of frames were collected with 0.50° steps in ω at four different φ settings and a detector position of −33° in 2θ. The intensity data were corrected for absorption,[27] and final cell constants were calculated from the *xyz* centroids of approximately 4000 strong reflections from the actual data collection after integration.[28] Structures were solved using SIR97[29] and refined using SHELXL-97.[30] Space groups were determined based on systematic absences, intensity statistics, and Cambridge Structural Database frequencies.[31] Direct-methods solutions were calculated which provided most non-hydrogen atoms from the difference Fourier map. Full-matrix least-squares (on F^2)/difference Fourier cycles were performed which located the remaining non-hydrogen atoms. Non-hydrogen atoms were refined with anisotropic displacement parameters, and hydrogen atoms were placed in ideal positions and refined as riding atoms with relative isotropic displacement parameters. All refinements were run to mathematical convergence.

Structure **4b** is a pentane and dichloromethane solvate. In structure **5** the atoms of the cation and one SbF_6 anion lie in general positions, while the second anion has two independent positions coincident with crystallographic 2-fold axes. While the co-crystallized dichloromethane solvent of **5** could be located and modeled, the *n*-hexane solvent was found highly disordered in channels and had to be removed from the model using program PLATON, function SQUEEZE,[32] which determined there to be 418 electrons in 5207 Å^3 removed per unit cell.

Acknowledgment. The authors thank the National Science Foundation (Grants CHE-0556225 and CHE-0847851) for support of this work.

Supporting Information Available: X-ray crystallographic data of **4b** and **5** in CIF format. This material is available free of charge via the Internet at http://pubs.acs.org.

(26) *APEX2*, version 1.0−22; Bruker AXS: Madison, WI, 2004.

(27) Sheldrick, G. M. *SADABS*, version 2008/1; University of Göttingen: Göttingen, Germany, 2008.

(28) *SAINT*, version 7.60A; Bruker AXS: Madison, WI, 2003.

(29) Altomare, A.; Burla, M. C.; Camalli, M.; Cascarano, G. L.; Giacovazzo, C.; Guagliardi, A.; Moliterni, A. G. G.; Polidori, G.; Spagna, R. *SIR97: A new program for solving and refining crystal structures*; Istituto di Cristallografia, CNR: Bari, Italy, 1999.

(30) Sheldrick, G. M. *Acta Crystallogr.* **2008**, *A64*, 112.

(31) Allen, F. *Acta Crystallogr.* **2002**, *B58*, 380.

(32) Spek, A. L. *PLATON: A multipurpose crystallographic tool*, version 300106; Utrecht University: Utrecht, The Netherlands, 2006.